Novel Amidino-Substituted Thienyl- and Furylvinylbenzimidazole: Derivatives and Their Photochemical Conversion into Corresponding Diazacyclopenta[*c*]fluorenes. Synthesis, Interactions with DNA and RNA, and Antitumor Evaluation. 4

Marijana Hranjec,[†] Ivo Piantanida,*,[‡] Marijeta Kralj,[§] Lidija Šuman,[§] Krešimir Pavelić,[§] and Grace Karminski-Zamola*,[†]

Department of Organic Chemistry, Faculty of Chemical Engineering and Technology, University of Zagreb, Marulićev trg 20, P.O. Box 177, HR-10000 Zagreb, Croatia, Division of Organic Chemistry and Biochemistry, "Rudjer Bošković" Institute, P.O. Box 180, HR-10002 Zagreb, Croatia, and Division of Molecular Medicine, "Rudjer Bošković" Institute, Bijenička cesta 54, P.O. Box 180, HR-10000 Zagreb, Croatia

Synthesis of novel nonfused amidino-substituted thienyl- and furylvinylbenzimidazole: derivatives and their photochemical cyclization into corresponding diazacyclopenta[*c*]fluorenes is described. All studied compounds showed prominent growth inhibitory effect. The fused compounds showed stronger activity than nonfused ones, whereby imidazolyl-substituted compound **11** proved to be the most active one. Besides, it induced strong G2/M arrest of the cell cycle followed by drastic apoptosis, which is in accordance with the DNA intercalative binding mode determined by the spectroscopic studies. Nonfused derivatives induced strong S phase arrest of the cell cycle followed by apoptosis that together with DNA minor groove binding mode pointed to topoisomerase I inhibition. In addition, all nonfused compounds revealed pronounced selectivity toward tumor cells in comparison with nontumor cells. On the basis of the presented results, both nonfused and fused thiophene-containing imidazolyl derivatives should be considered as promising lead compounds for further investigation.

Introduction

In spite of great advances in cancer therapy, there has been tremendous growth in recent years in the number and types of new anticancer agents, with an emphasis on creating new DNA-active drugs.[1–3] Most of the presently used anticancer drugs interact with DNA noncovalently by two main binding modes: (a) DNA minor groove binding through a combination of hydrophobic, electrostatic, and hydrogen bonding interactions and (b) intercalative binding in which a planar aromatic moiety slides between the DNA base pairs.[4–6] The interactions of chemotherapeutics with the DNA can cause changes in the physiological functions of DNA, and therefore, understanding the interactions of small molecules with DNA is of significance in the rational design of more powerful and selective anticancer agents.[7,8]

The benzimidazole unit is the key building block for a variety of derivatives that are known to play crucial roles in the functions of a number of biologically important molecules.[9] In addition, the constant and growing interest over the past few years for the synthesis and biological studies of substituted benzimidazoles and their azino fused derivatives is owed partly to their well-known biological activities such as anticancer,[10–14] antimicrobial,[15–17] antiviral,[10,18–20] antihistaminic,[21,22] and antifungal activities.[23,24]

Furthermore, amidines are structural parts of numerous compounds of biological interest including important medical and biochemical agents.[6,25–27] The amidine groups at the termini of the molecule seemed to contribute significantly to the complex stability between the dications and the DNA through H-bonding and electrostatic interactions.[1,6] However, quite often diarylamidines aggregate within the DNA grooves; for example, phenylfuranbenzimidazole diamidine binds to AT-rich sequences as a monomer while to GC-rich sequences bind as dimers.[28] Pentamidine, the minor groove binding agent, has been successfully used in the clinic treatment of human parasitic diseases.[29] Phenylthiophenebenzimidazole diamidines showed 10-fold increased affinity for the minor groove binding at AT sequences.[30]

As a part of our medicinal chemistry project aimed at the synthesis of potential anticancer agents, we have prepared amidino-substituted styryl-2-benzimidazoles and their fused benzimidazo[1,2-*a*]quinoline derivatives.[31] The most active imidazolyl-substituted fused derivative inhibited topoisomerase II and induced strong G2/M cell cycle arrest, pointing to the impairment in mitotic progression. Its pronounced selectivity toward colon carcinoma cells encouraged further development of this compound as a lead. The nonfused derivatives showed a different interaction with DNA and pronounced selectivity toward tumor cells in regard to normal cells. These results prompted us to synthesize heterocyclic furyl- and thienyl-substituted analogues of the above-mentioned compounds. In this work we present the synthesis of *E-N*-substituted-2-(2-thiophen-2-ylvinyl)-3*H*-benzimidazole-5(6)-carboxamidine hydrochlorides **2−5**, *E*-2-(2-furan-2-ylvinyl)-*N*-substituted-3*H*-benzimidazole-5(6)-carboxamidine hydrochlorides **6−9**, and *N*-substituted 3-thia-6,10b-diazacyclopenta[*c*]fluorene-8(9)-carboxamidine hydrochlorides **10−13** (Figure 1), detailed study of their interactions with DNA/RNA, and antiproliferative activity on a panel of tumor cell lines.

Synthesis

Novel *E-N*-substituted 2-(2-thiophen-2-ylvinyl)-3*H*-benzimidazole-5(6)-carboxamidines hydrochlorides **2−5** and *E*-2-(2-furan-2-ylvinyl)-*N*-substituted-3*H*-benzimidazole-5(6)-carbox-

* To whom correspondence should be addressed. For I.P.: phone, +385 1 4561 111/1306; fax, +3851 4680 195; e-mail, pianta@irb.hr. For G.K.-Z.: phone, ++38514597215; fax, ++38514597250; e-mail, gzamola@pierre.fkit.hr.

† University of Zagreb.

‡ Division of Organic Chemistry and Biochemistry, "Rudjer Bošković" Institute.

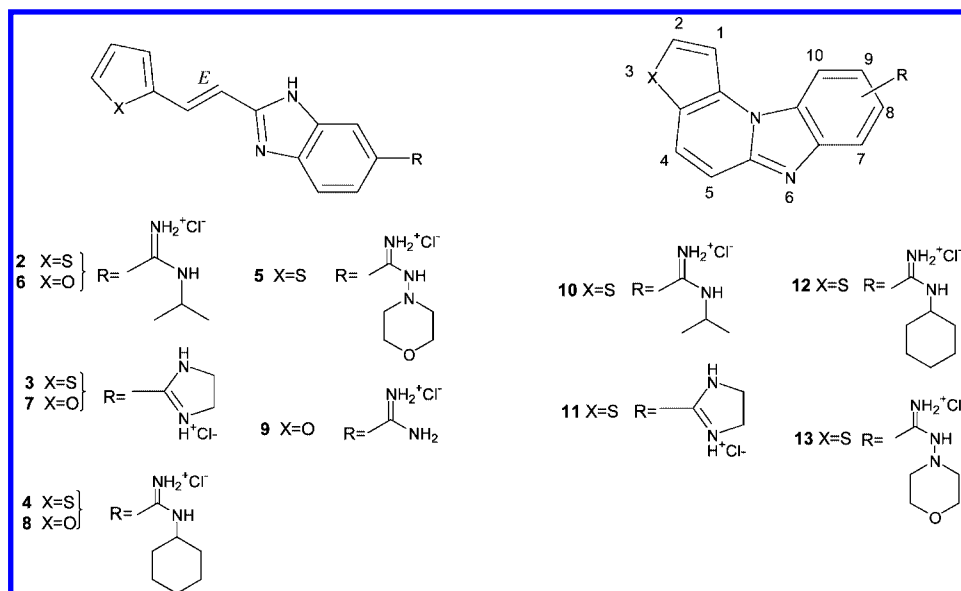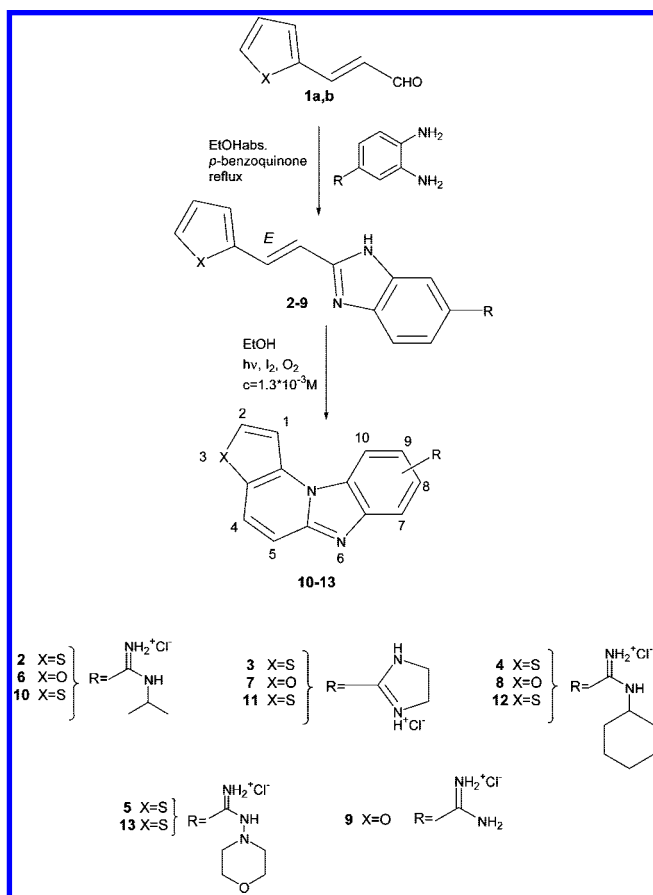§ Division of Molecular Medicine, "Rudjer Bošković" Institute.

Figure 1. Structures of the studied compounds.

Scheme 1. Synthetic Procedures for the Amidino-Substituted *E*-2-(2-Thiophen-2-ylvinyl)-3*H*-benzimidazoles **2–5**, *E*-2-(2-Furan-2-ylvinyl)-3*H*-benzimidazoles **6–9**, and 3-Thia-6,10b-diazacyclopenta[*c*]fluorenes **10–13**

amidines hydrochlorides **6–9** were prepared by the condensation reaction of 3-thiophen-2-ylpropenal and 3-furan-2-ylpropenal **1a,b** with the corresponding, earlier prepared 4-*N*-amidino-substituted 1,2-phenylenediamines and *p*-benzoquinone in 50–88% yield (Scheme 1). 4-*N*-Amidino-substituted 1,2-phenylenediamines were prepared from cyano-substituted derivatives in the Pinner reaction, using the earlier described

methods. Novel *N*-substituted-3-thia-6,10b-diaza-cyclopenta[*c*]-fluorene-8(9)-carboxamidine hydrochlorides **10–13** were prepared by photochemical dehydrocyclization of ethanolic solution ($c = 1.3 \times 10^{-3}$ mol dm^{-3}) of *E*-*N*-substituted-2-(2-thiophen-2-ylvinyl)-3*H*-benzimidazole-5(6)-carboxamidines hydrochlorides **2–5** in 67–80% yield as a mixture of two inseparable structure isomers. Photochemical dehydrocyclization of amidino-substituted *E*-2-(2-furan-2-ylvinyl)-3*H*-benzimidazoles **6–9** did not give the desired fused products.

All structures of novel nonfused **2–9** and fused derivatives **10–13** were determined by NMR analysis, based on the analysis of H–H coupling constants as well as chemical shifts. In ^{1}H NMR spectra of all nonfused derivatives **2–9**, two doublets for *trans*-ethylenic protons with coupling constants of ~16 Hz can be observed. The photocyclization reaction leads to a downfield shift of the signal of the ethylenic proton and most other protons. Proton of NH group of benzimidazole ring and one proton of thiophene ring disappeared, thus confirming fused structure formation. Doublets for two protons on fluorene ring, with coupling constants of ~9.5 Hz, can be observed, and these values are characteristic for this type of fused compound.

Spectroscopic Properties of Studied Compounds

Compounds studied in this paper could be divided in two groups: "non-fused" derivatives (Figure 1, **2–9**) and their "fused" photoproducts (Figure 1, **10–13**). Because of the structural similarity, we have chosen to study compounds **3**, **4**, and **8** as representatives of the "nonfused" derivatives and compounds **11** and **12** as representatives of "fused" derivatives. Since for DNA binding studies of the above-mentioned compounds application of spectrophotometric methods was necessary, we have characterized their aqueous solutions by means of electronic absorption (UV/vis) and fluorescence emission spectra (Table 1).

Absorbencies of aqueous solutions of compounds are proportional to their concentrations in the range 2×10^{-6} to 2×10^{-5} mol dm^{-3} and also did not change significantly with a temperature increase up to 90 °C. These observations indicated that there is no significant intermolecular stacking, which should give rise to hypochromicity effects. Aqueous solutions of all studied compounds were shown to be stable over a longer period. The "nonfused" derivatives **3**, **4**, and **8** exhibited rather

Table 1. Electronic Absorption Maxima and Corresponding Molar Extinction Coefficients of Studied Compounds in Water, Fluorescence Emission Maxima, and Corresponding Relative Quantum Yield $(Q)^a$

compd	absorption maxima		fluorescence emission	
	λ_{max}, nm	$\varepsilon \times 10^3$, dm^3 mol^{-1} cm^{-1}	λ_{max}, nm	^aQ
3	356	30.3	418	<0.1
4	351	32.2	426	<0.1
8	348	35.5	421	<0.1
11	273	21.8		
	370	9.6	437	0.85
	386	7.9		
12	265	28.4		
	364	12.8	419	0.84
	382	9.5		

^{a} Relative quantum yield (Q) was determined with respect to standard *N*-acetyl-L-tryptophanamide (NATA) $Q = 0.14$.

weak fluorescence, while the emission of their "fused" analogues **11** and **12** was exceptionally strong, allowing measurements even at 10 nM concentrations. Fluorescence emissions of all studied compounds (**3**, **4**, **8**, **11**, **12**) were proportional to their concentration in the range 1×10^{-7} to 5×10^{-6} mol dm^{-3}.

Interactions of Compounds 3, 4, 8, 11, 12 with Double Stranded (ds-) DNA and (ds-) RNA

UV/Visible Titrations. The UV/vis spectra of compounds **3**, **4**, **8**, **11**, **12** exhibited strong hypochromic changes upon titration with ct-DNA (Figure 2A,B, Table 2), as well as during titrations with several ds-RNAs (Figure 2C,D, Table 2). While for most compounds addition of ct-DNA induced pronounced batochromic shifts of the absorption maxima (Figure 2A,B, Table 2), the shifts of the absorption maxima of studied compounds in titrations with ds-RNA ($\Delta\lambda$, Table 2) were strongly dependent on both the compound structure and base pair type in the polynucleotide. It is interesting to note that polyG−polyC exclusively induced hypsochromic shifts of absorption maxima of some "non-fused" derivatives (**3** and **4**, Table 2). Such pronounced changes of UV/vis spectra pointed toward involvement of the studied compounds in strong π−π aromatic stacking interactions, although it is not possible to distinguish between interactions of studied compounds with ds-polynucleotide and interactions between molecules of compound (e.g., molecule agglomeration within the grooves of polynucleotide).

The major spectroscopic changes were observed at excess of compound over polynucleotide. At such conditions more different binding modes could be present,[1,32] which is strongly supported for **3** by spectral changes in opposite directions (Figure 2A,B). Therefore, it was not possible to process UV/vis titration data by the Scatchard equation to obtain binding constants.[33]

Fluorimetric Titrations. Strong fluorescence of the studied compounds in aqueous media allowed titrations to be done exclusively at high excess of DNA/RNA over compound. Addition of any double-stranded polynucleotide strongly quenched fluorescence of "fused" analogues **11** and **12** (Figure 3B, Table 3). It is noted that in contrast to "fused" compounds, addition of both ds-DNA and ds-RNA compounds induced strong fluorescence increase of "non-fused" analogues **3**, **4**, and **8** (Figure 3A, Table 3). That could be attributed to the increased rigidity of the double bond of **3**, **4**, and **8** upon binding to the double helix, thus forcing planar conformation of otherwise flexible molecule, which could result in a strong increase of fluorescence emission for the same reason as proposed for cyanine dyes; namely, the huge enhancement of fluorescence quantum yield of cyanine dyes upon binding to DNA is believed

to originate from the loss of mobility around the methine bridge connecting the quinoline and benzoxazole, respectively, and benzothiazole moieties due to the constrictive DNA environment. In the free form, isomerization around this bridge is an important nonradiative decay channel of the photoexcited dye molecule, whereas upon intercalation, large amplitude motion of the probe is strongly hindered.[34] Only fluorescence of **4** was similarly enhanced by both polyA−polyU and polyG−polyC, while for all other compounds (**3**, **8**, **11**, **12**) fluorescence change (enhancement or quenching) was significantly more pronounced upon addition of polyA− polyU than polyG−polyC (Table 3).

Processing of the fluorimetric titration data by Scatchard equation[33] gave binding constants (log K values) (Table 3). Obtained binding constants depend significantly on the compound structure, as well as on the base pair type in the polynucleotide. The affinity of "fused" derivatives (**11**, **12**) toward ct-DNA is somewhat higher than the affinity of "non-fused" analogues (**3**, **4**, **8**), but this preference is not obvious for the ds-RNA polynucleotides. Furthermore, fluorimetric titrations of some "nonfused" analogues with polyG−polyC (**3**) and with both ds-RNAs (**8**) pointed toward simultaneous formation of more different complexes, thus hampering the calculation of binding constants.[1,32]

Thermal Denaturation Experiments. In the thermal denaturation experiments (Table 4) addition of "nonfused" analogues (**3**, **8**) yielded only weak but comparable stabilization of both ct-DNA and polyA−polyU. On the other hand, "nonfused" compound **4** yielded weak stabilization of exclusively ct-DNA. The "fused" derivatives **11** (Figure 4) and **12** stabilized ct-DNA and polyA−polyU significantly more strongly than their "nonfused" analogues (**3** and **4**, respectively).

More detailed study of thermal stabilization of ct-DNA/ compound complexes revealed strongly nonlinear dependence of ΔT_m values on the ratio r, suggesting for all compounds saturation of binding sites at $r = 0.2-0.3$, which is in good agreement with the values of Scatchard ratio n obtained from fluorimetric titrations (Table 3).

CD Experiments. So far, noncovalent interactions at 25 °C were studied by monitoring the spectroscopic properties of studied compound upon addition of the polynucleotides. In order to get insight into the changes of polynucleotide properties induced by small molecule binding, we have chosen CD spectroscopy as a highly sensitive method toward conformational changes in the secondary structure of polynucleotides.[35] In addition, achiral small molecules like **3**, **4**, **8**, **11**, and **12** can eventually acquire induced CD spectrum (ICD) upon binding to polynucleotides, from which mutual orientation of small molecule and polynucleotide chiral axis could be derived, consequently giving useful information about modes of interaction.[35]

Addition of "nonfused" derivatives (**3**, **4**, **8**) resulted in a decrease of intensity of the ct-DNA CD spectrum (Figure 5). Additionally, strong positive induced CD (ICD) band between $\lambda = 350$ and 400 nm appeared. Since "nonfused" analogues do not have any intrinsic CD spectrum, ICD band most likely resulted from the binding of **3**, **4**, and **8** into the minor groove of ct-DNA.[36,37]

In contrast to "nonfused" compounds **3**, **4**, and **8**, addition of their "fused" analogues (**11**, **12**) to ct-DNA did not yield induced CD (ICD) band between $\lambda = 350$ and 400 nm, thus excluding binding into the minor groove of ct-DNA as a dominant interaction.[36,37] Surprisingly, changes of the negative ($\lambda = 245$ nm) and positive ($\lambda = 278$ nm) band of the ct-DNA induced by titration with "fused" derivatives (**11**, **12**) were different
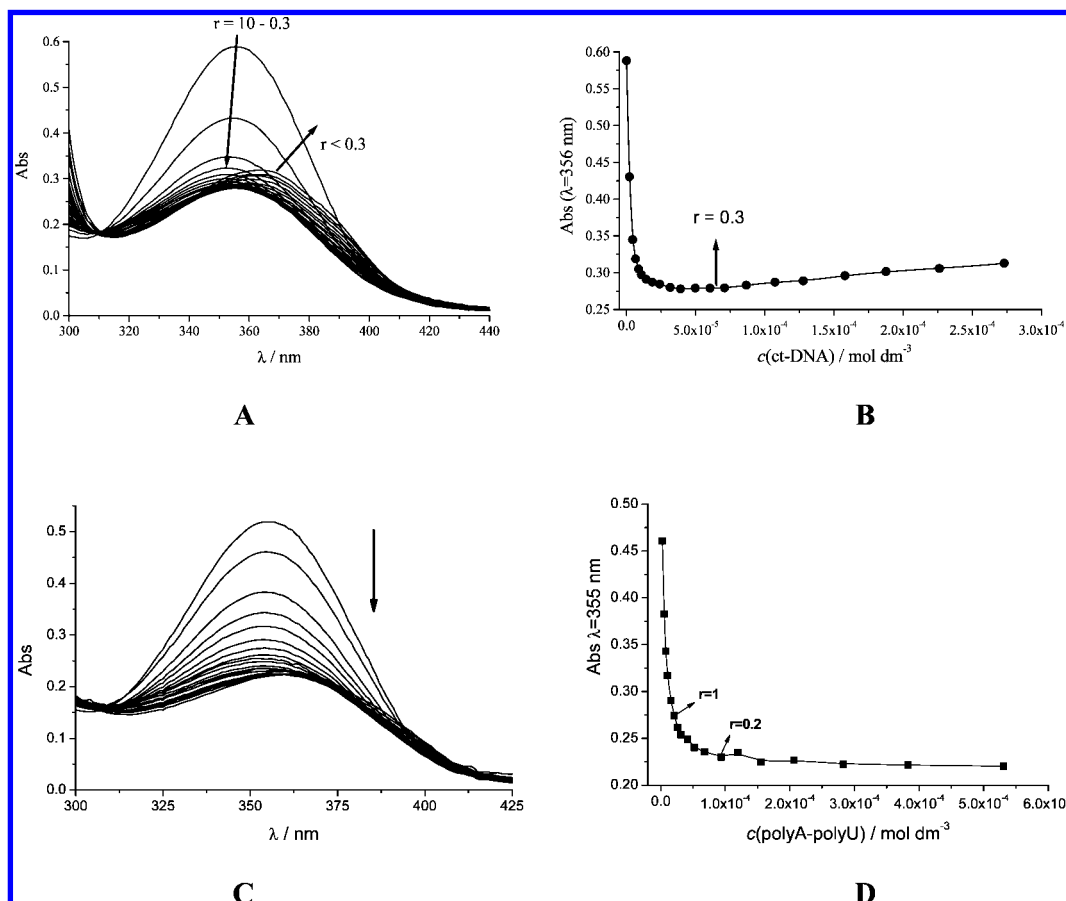
Figure 2. UV/vis titration of **3** ($c = 2.0 \times 10^{-5}$ mol dm^{-3}) with ct-DNA (A). Spectroscopic changes at $\lambda_{max} = 356$ nm as a function of ct-DNA concentration (B). UV/vis titration of **3** ($c = 2.0 \times 10^{-5}$ mol dm^{-3}) with polyA−polyU (C). Spectroscopic changes at $\lambda_{max} = 356$ nm as a function of polyA−polyU concentration (D). Experiments were done at pH 7.0, with buffer Na cacodylate, $I = 0.05$ mol dm^{-3}, ratio $r = $ [**3**]/[polynucleotide].

Table 2. Changes in the UV/Visible Spectra of **3**, **4**, **8**, **11**, **12** upon Titration with Double-Stranded DNA and RNA (pH 7, Na Cacodylate Buffer, $I = 0.05$ M)

	3	**4**	**8**	**11**	**12**
			ct-DNA		
$\Delta\lambda_1$,[a] nm	+11	0	+13	+13	+8
$\Delta\lambda_2$,[a] nm				+15	+7
H, %	c	46 (351 nm)	42 (348 nm)	39 (370 nm)	54 (364 nm)
			polyA−polyU		
$\Delta\lambda_1$,[a] nm	+4	0	0	+13	0
$\Delta\lambda_2$,[a] nm				+15	0
H,[b] %	30 (356 nm)	21 (351 nm)	23 (348 nm)	35 (370 nm)	17 (364 nm)
			polyG−polyC		
$\Delta\lambda_1$,[a] nm	−5	−5	0	+13	0
$\Delta\lambda_2$,[a] nm				+15	0
H,[b] %	40 (356 nm)	30 (351 nm)	6 (348 nm)	39 (370 nm)	13 (364 nm)

[a] Shift of the absorbance maximum, $\Delta\lambda = \lambda$(complex) $- \lambda(x - y)$. Absorbance maxima λ_1: **8**, $\lambda = 348$ nm; **4**, $\lambda = 351$ nm; **3**, $\lambda = 356$ nm; **12**, $\lambda = 364$ nm; **11**, $\lambda = 370$ nm. Absorbance maxima λ_2: **12**, $\lambda = 382$ nm; **11**, $\lambda = 384$ nm. [b] Hypochromic effect, $H = $ (Abs(compound) $-$ Abs(complex))/(Abs(compound)) $\times$ 100. Values of Abs(complex) are estimated by nonlinear extrapolation. [c] Absorbance changes in opposite direction (Figure 2): Abs decrease for $r = 10-0.3$ followed by Abs increase for $r < 0.3$.

(Figure 5). The intensity of the negative band ($\lambda = 245$ nm) substantially decreased upon each addition of **11**, **12**, and the dependence of change on the ratio $r_{[11,12]/[ct-DNA]}$ was strongly nonlinear, suggesting the saturation of binding sites at $r = 0.2-0.3$, similar to that found in the fluorimetric and thermal denaturation experiments. On the other hand, intensity of the positive band ($\lambda = 278$ nm) weakly increased for $r_{[11,12]/[ct-DNA]} = 0-0.3$ and then decreased for $r > 0.3$, such opposite spectral changes pointing toward presence of more than two spectroscopicaly active species. The experimental conditions (ratio r,

concentrations of **11**, **12**, and ct-DNA) of CD titrations are comparable with UV/vis titrations, the last showing coexistence of more binding modes. Since the strongest absorbance maximum of **11** and **12** (Table 2) is positioned close to the CD band of ct-DNA ($\lambda = 278$ nm), most likely different combinations of binding modes resulted in different changes of CD spectrum at various ratios r. Obviously, that did not influence significantly the changes of the negative ct-DNA band ($\lambda = 245$ nm).

The CD titrations of ds-RNA (polyA−polyU, Supporting Information) with **3**, **4**, **8**, **11**, and **12** yielded results substantially
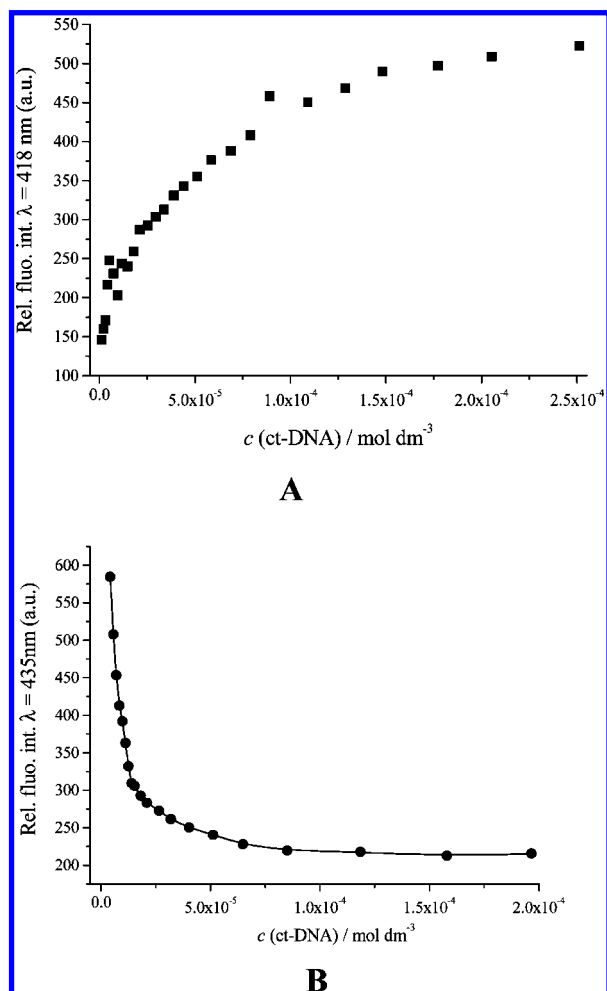
Figure 3. Fluorimetric titration with ct-DNA of (A) "nonfused" compound **3**, $c = 8.7 \times 10^{-7}$ mol dm^{-3}, $\lambda_{exc} = 358$ nm, $\lambda_{emiss} = 418$ nm, $t_{incub} = 6$ min, and (B) "fused" compound **11**, $c = 5.8 \times 10^{-7}$ mol dm^{-3}, $\lambda_{exc} = 370$ nm, $\lambda_{emiss} = 435$ nm, $t_{incub} = 7$ min.

Table 3. Binding Constants (log K Values) and Ratios $n_{[\text{bound compound}]/[\text{polynucleotide phosphate}]}$[a] Calculated from the Fluorimetric Titrations with Polynucleotides at pH 7.0 (Buffer Na Cacodylate, $I = 0.05$ mol dm^{-3})

	ct-DNA		polyA–polyU		polyG–polyC	
	log K	Int/Int$_0$ [b]	log K	Int/Int$_0$ [b]	log K	Int/Int$_0$ [b]
3	5.0	4	5.8	5.3	5.6[d]	1.3
4	5.2	10	4.5	4.8	4.6	4.5
8	5.2	9	c	0.9/>10	e	e
11	6.7	0.2	6.1	0.8	5.3	0
12	6.0	0.3	5.0	0.6	4.3	0.3

[a] Processing of titration data by means of Scatchard equation[33] gave ratio $n_{[\text{bound compound}]/[\text{polynucleotide}]} = 0.3-0.1$. For easier comparison, all log K values were recalculated for fixed $n = 0.2$. [b] Int$_0$: starting fluorescence intensity of compound. Int: fluorescence intensity of compound/polynucleotide complex calculated by Scatchard equation. [c] Fluorimetric changes in opposite direction hampered processing by Scatchard equation:[33] emission decrease for $r = 2-0.2$ followed by emission increase for $r < 0.2$. [d] The cumulative binding constant for mixed binding modes, calculated Scatchard ratio $n = 2$. [e] Small fluorescence changes didn't allow accurate calculation.

different from those obtained in experiments with ct-DNA (Figure 5). Additions of **8** did not yield any significant change in the CD spectrum of polyA–polyU, while additions of **3**, **11**, and **12** caused only a minor decrease of intensity of RNA CD spectra. Only **4** yielded a somewhat stronger decrease of intensity of polyA–polyU CD band at 265 nm. Quite the opposite to the experiments with ct-DNA, in the experiments with polyA–polyU no ICD bands at $\lambda > 300$ nm were observed.

Table 4. ΔT_m Values[a] of ct-DNA and polyA–polyU upon Addition of Different Ratios r [b] of Studied Compounds at pH 7.0 (Buffer Na Cacodylate, $I = 0.05$ mol dm^{-3})

r [b]	ΔT_m, °C				
	3	4	8	11	12
		ct-DNA			
0.1	1.3	0	1.0	1.7	1.4
0.2	1.3	1.0	1.6	3.2	2.2
0.3	1.4	1.1	1.5	4.3	3.9
		polyA–polyU			
0.3	2.2	0	1.6	3.4	2.4

[a] Error in ΔT_m: ±0.5 °C. [b] $r =$ [compound]/[polynucleotide].

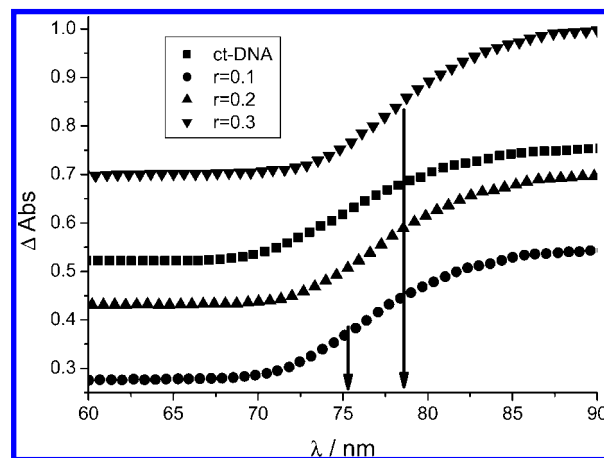**Figure 4.** Thermal denaturation curves of ct-DNA and **11** at pH 7 (sodium cacodylate buffer, $I = 0.05$ mol dm^{-3}). For measuring conditions, see footnotes to Table 4 and the Experimental Section. The ratio r ([**11**]/[ct-DNA]) values are 0.0, 0.1, 0.2, 0.3 (from bottom curve up), and the curves are normalized.

Viscometry. Viscometry experiments (Supporting Information) yielded values of $\alpha(\mathbf{11}) = 0.92$ and $\alpha(\mathbf{12}) = 0.74$, which differ from the value obtained for ethidium bromide ($\alpha(\text{EB}) = 0.83$) by the error of the method ($\alpha \pm 0.1$). Obtained values strongly support intercalation of **11** and **12** into ds-DNA as the dominant binding mode. On the other hand, addition of "nonfused" analogues (**3**, **4**) resulted only in minor changes of DNA solution viscosity ($\alpha(\mathbf{3,4}) < 0.1$), thus pointing that intercalative binding mode is not dominant interaction of "nonfused" compounds with ds-DNA.

Discussion of the DNA/RNA Binding Studies of Compounds 3, 4, 8, 11, 12

The "fused" derivatives (**11** and **12**) exhibited somewhat higher affinity (log K values) and significantly stronger ΔT_m values compared to their "nonfused" analogues (**3** and **4**, respectively). All methods pointed toward saturation of binding sites at $r_{[\mathbf{11,12}]/[\text{polynucleotide}]} = 0.2-0.3$. The absence of a strong positive ICD effect excluded the binding of **11** and **12** into ct-DNA minor groove.[36,37] The absence of the weak negative ICD effect at long wavelengths, which is expected for intercalators, can be explained in several ways, the most probable being orientation heterogeneity of intercalated molecules.[35–37] Viscometry results strongly supported intercalation of **11** and **12** as a dominant interaction with ds-DNA. Taking into account the large, planar aromatic surface, intercalation into ds-DNA and ds-RNA is the most probable binding mode for **11** and **12**.

According to the strong positive ICD bands,[36,37] as well as moderate affinity and weak thermal stabilization effects (due to only one positive charge), the "nonfused" analogues (**3**, **4**,
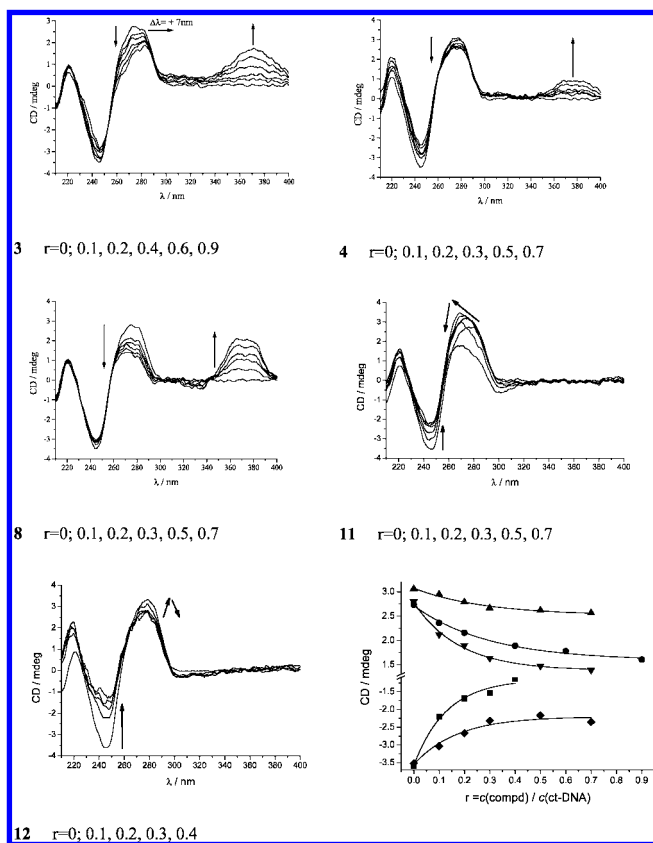
Figure 5. CD spectra of ct-DNA ($c = 2.0 \times 10^{-5}$ mol dm^{-3}) with **3**, **4**, **8**, **11**, and **12** at different ratios $r =$ [compound]/[ct-DNA] (pH 7.0, buffer Na cacodylate, $I = 0.05$ mol dm^{-3}). Bottom right: changes of ct-DNA CD signal at chosen wavelength with respect to ratio r. For nonfused compounds, $\lambda = 275$ nm, **3** (●), **4** (▲), **8** (▼). For fused compounds, $\lambda = 245$ nm, **11** (◆) and **12** (■).

8) bind most likely into the minor groove of the ct-DNA.[1,29,38] However, compounds **3** and **8** yielded weak thermal stabilization of polyA−polyU, thus suggesting intercalation into ds-RNA at least as one mode of interaction. Such a switch of binding mode (ds-DNA minor groove binding, ds-RNA intercalation) was earlier observed for several groups of compounds quite closely related to the here-studied "nonfused" derivatives.[38]

Biological Results and Discussion

Compounds **2**−**13** were tested for their potential antiproliferative effects on a panel of six human cell lines, five of which were derived from different cancer types including HeLa (cervical carcinoma), MCF-7 (breast carcinoma), SW620 (colon carcinoma), MiaPaCa-2 (pancreatic carcinoma), Hep-2 (laryngeal carcinoma), and one from normal diploid fibroblasts, WI 38 (Table 5 and Figure 6).

All tested compounds showed prominent growth inhibitory effect. There are several important points to emphasize: (i) in general all fused compounds are more active (showing nondifferential and cytotoxic effect) than nonfused ones; (ii) imidazolyl-substituted compound **11** proved to be the most active one; (iii) HeLa and MCF-7 cells were the most sensitive to all tested compounds; (iv) nonfused compounds containing the thiophene moiety (**2**−**5**) were significantly more active than their furan-containing analogues (**6**−**9**). Although the activities of tiophene nonfused derivatives are overall comparable, it is pointed out that only compound **2** did not show significant activity toward normal cells.

Table 5. In Vitro Inhibition of Compounds **2**−**13** on the Growth of Tumor Cells and Normal Human Fibroblasts (WI 38)

compd	IC$_{50}$,[a] μM					
	Hep-2	HeLa	MiaPaCa-2	SW620	MCF-7	WI 38
2	12 ± 2	7 ± 3	11 ± 6	>100	4 ± 2	>100
3	11 ± 2	5 ± 0.9	10 ± 2	11 ± 0.6	3 ± 0.9	29 ± 2
4	9 ± 5	4 ± 1	6 ± 3	12 ± 5	2 ± 0.08	33 ± 5
5	7 ± 5	3 ± 0.6	12 ± 2	12 ± 5	10 ± 6	13 ± 5
6	>100	20 ± 19	>100	>100	62 ± 15	>100
13	7 ± 3	7 ± 0.3	9 ± 5	3 ± 0.5	6 ± 1	8 ± 7
7	67 ± 5	10 ± 5	51 ± 10	50 ± 9	9 ± 0.6	>100
8	65 ± 30	6 ± 2	78 ± 4	>100	19 ± 4	>100
9	19 ± 16	4 ± 0.3	>100	16 ± 6	12 ± 4	>100
10	17 ± 4	12 ± 0.06	16 ± 4	19 ± 7	12 ± 0.2	18 ± 7
11	3 ± 0.3	3 ± 0.3	3 ± 0.7	2 ± 0.4	2 ± 0.3	3 ± 0.03
12	4 ± 2	3 ± 0.2	4 ± 0.3	4 ± 0.01	3 ± 1	9 ± 2

[a] IC$_{50}$: the concentration that causes a 50% reduction of the cell growth.
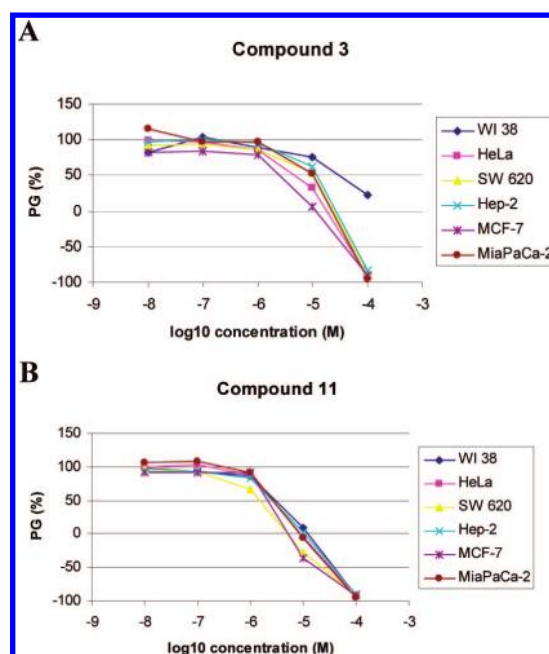

Figure 6. Concentration−response profiles for the representative nonfused (**3**) and fused (**11**) analogues tested on various human cell lines in vitro. The cells were treated with the compounds at different concentrations, and percentage of growth (PG) was calculated. Each point represents a mean value of four replicates in three individual experiments.

Very similar effects were noticed in our previous study on the antiproliferative action of amidino-substituted styryl-2-benzimidazoles and benzimidazo[1,2-*a*]quinolines,[31] whereby the imidazolyl-substituted benzimidazoquinoline was the most active compound and HeLa and MCF-7 cells showed greater sensitivity.

Considering the above-mentioned DNA/RNA binding data and similar biological activity to the previously published results,[31] we assumed that the mechanisms of action of these compounds should also be similar (namely, noncovalent interactions with cellular DNA), inducing cell cycle disturbances and mitotic impairment. Therefore, we performed additional experiments in order to gain closer analysis of the mechanisms of tumor cell proliferation inhibition or death.

Cell Cycle Perturbations and Apoptosis Induction. We selected the fused compound **11** and its nonfused analogue **3** as the representatives of the most active compounds to investigate their influence on the MiaPaCa-2 cell cycle after 24, 48, and 72 h treatment periods (Figure 7). Obtained results
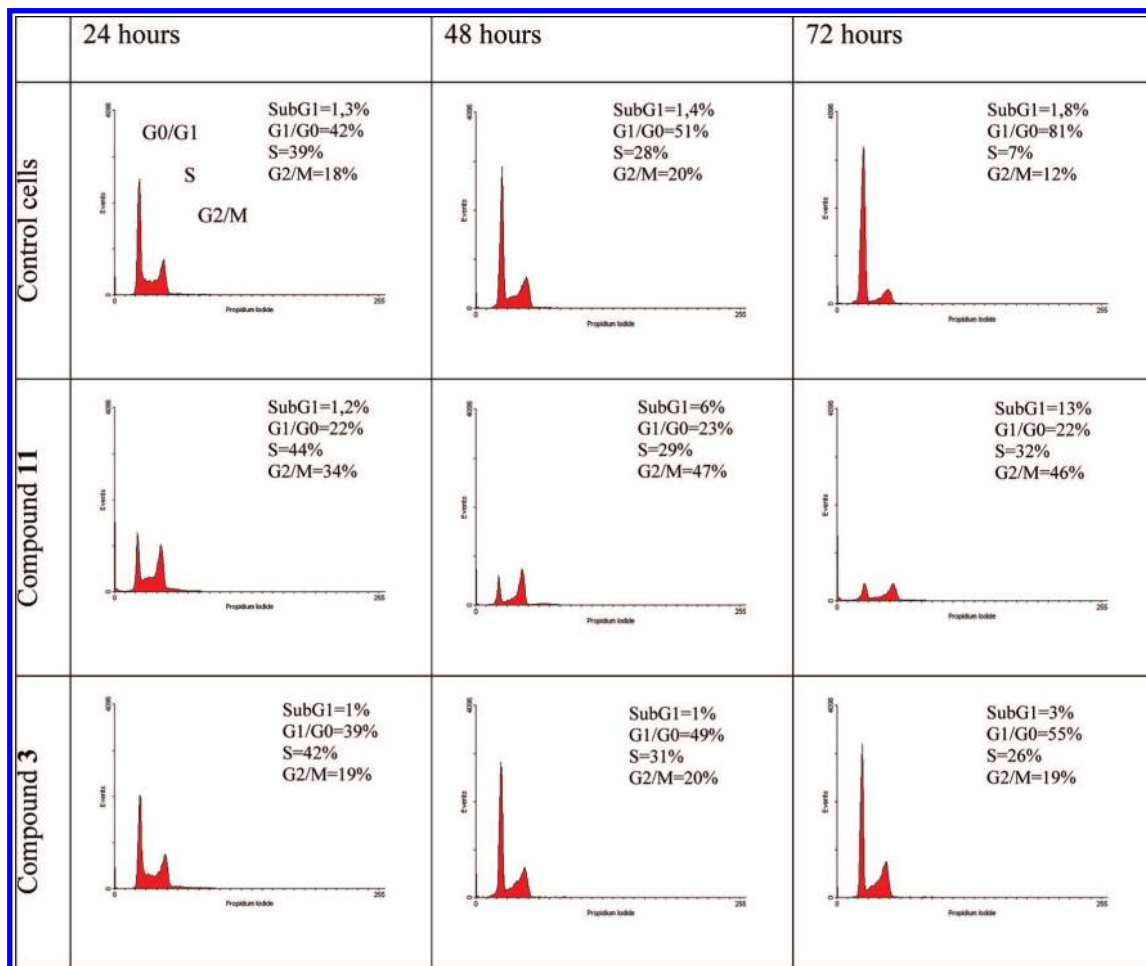
Figure 7. DNA histograms obtained by flow cytometry (see materials and methods section), and the percentages of cells in sub G1 (apoptotic cells), G0/G1, S, and G2/M cell cycle phase, after the treatment of MiaPaCa-2 cells with **11** and **3** (both at 10 μM) for 24, 48, and 72 h.

Table 6. Percentage of Cells Undergoing Apoptosis Induced by Compounds **3**, **4**, **11**, and **12** in MiaPaCa-2 and HeLa Cells after 72 h

| | | apoptotic cells, % | | | | | | | |
| | | **3** | | **4** | | **11** | | **12** | |
treatment	control, 0 μM	5 μM	10 μM	5 μM	10 μM	5 μM	10 μM	5 μM	10 μM
MiaPaCa-2	2 ± 2	2 ± 0	4 ± 0	3 ± 2	6 ± 3	11 ± 2	46 ± 4	5 ± 3	12 ± 8
HeLa	8 ± 4	8 ± 0	14 ± 2	13 ± 8	17 ± 3	27 ± 10	47 ± 20	10 ± 4	27 ± 14

clearly showed that at the concentration of 10 μM, both compounds initially induced statistically significant accumulation of cells in S phase and reduction of the G1 phase. The nonfused compound **3** arrested the cells mostly in the S phase throughout the entire treatment period, while fused compound **11** induced additional drastic G2/M phase arrest of the cell cycle that persisted over all three treatment periods and was accompanied by the accumulation of cells in the sub-G1 phase (apoptotic cells). There are two possible explanations for these different outcomes: the most important reason is certainly different DNA binding modes of **3** compared to **11**, whereby **3** binds preferentially to the DNA minor groove, while **11** intercalates into ds-DNA. Minor groove binders, in particular benzimidazoles and terbenzimidazoles, were shown to be powerful DNA topoisomerase I inhibitors.[1,7,39] Moreover, topoisomerase inhibitors induce S-phase arrest especially following prolonged exposure to low doses of compounds,[40,41] which was the case in our experiments. On the other hand, the intercalative mode of DNA binding along with somewhat higher concentration of **11** in regard to its IC$_{50}$ concentration (3 and 10 μM for **11**

and **3**, respectively), induced different and/or more pronounced DNA damage that induced apoptosis and consequently showed more striking activity. Namely, the difference between minor groove binders (**3**) and intercalators (**11**) resulted in different affinity toward DNA and different stabilization of ds-DNA helix, and in addition, only intercalation could cause unwinding and extension of DNA double helix.[1] Very similar results were obtained in our previous study with imidazolyl-substituted styryl-2-benzimidazoles and benzimidazo[1,2-*a*]quinolines that could be considered as nonfused and fused analogues to the here presented **3** and **11**, respectively, except that the here-presented benzimidazolethiophene (**3**) has much more pronounced activity than its benzimidazolestyryl analogue.[31]

Induction of Apoptosis. Since the sub-G1 fraction of cells is not quite a sensitive method of apoptosis detection, a more precise test should be used. Therefore, we assessed the annexin V assay to confirm the induction of apoptosis (Table 6). Besides **3** and **11**, we also tested additional two nonfused and fused compound analogues (**4** and **12**) having a cyclohexyl substituent. The results again confirmed that the imidazolyl-substituted
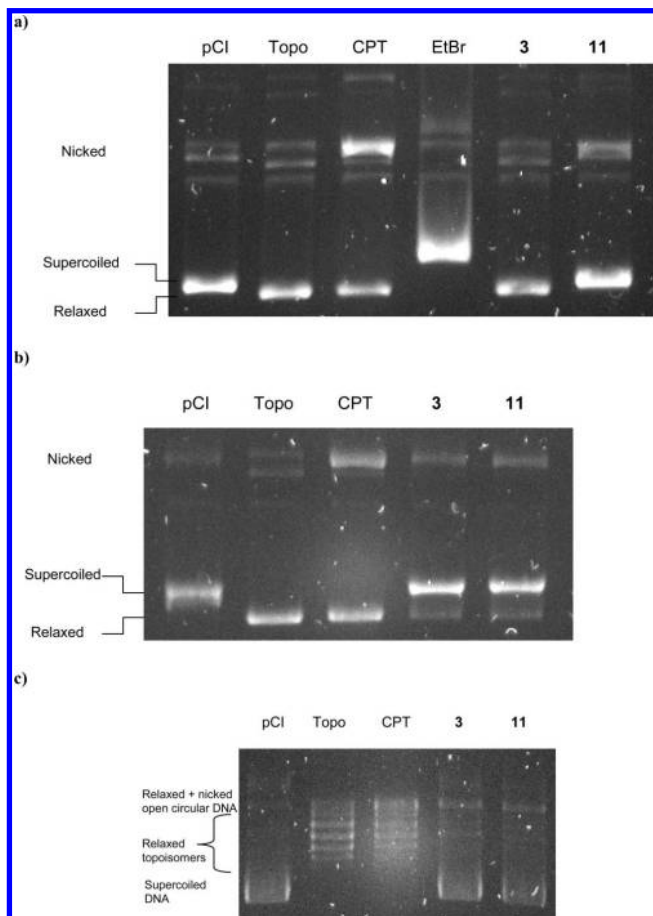
Figure 8. Influence of selected test compounds on relaxation of plasmid DNA by topoisomerase I. DNA samples were separated by electrophoresis on an agarose gel containing ethidium bromide (a, b) or without ethidium bromide (c). Shown are native supercoiled pCI DNA (0.4 μg) substrate in the assay buffer alone (lane pCI), incubated with topoisomerse I (4 U) (lane Topo) or in combination with control drug and camptothecin (100 μM) (lane CPT), ethidium bromide (10 μM) (lane EtBr), and selected test compounds **3** (100 μM (a) and 200 μM (b, c) and **11** (100 μM (a−c) (lanes **3** and **11**).

compound **11** had most drastic influence on the apoptosis induction in both HeLa and MiaPaCa-2 cells and was the only compound capable of inducing apoptosis at 5 μM concentration. HeLa cells were exceptionally sensitive also at lower (5 μM) concentration and even after 24 h of incubation (data not shown), which is in accordance with the growth inhibition results (Table 5). Interestingly, nonfused compounds **3** and **4** did not induce apoptosis in MiaPaCa-2 cells, but significant proportion of HeLa cells died by apoptosis after the treatment with **3** at 10 μM concentration, confirming again the growth inhibition results.

Topoisomerase I Unwinding/Cleavage Assay. To ascertain the previously mentioned assumption that tested compounds act as topoisomerase inhibitors, we employed in vitro assay using purified topoisomerase I from calf thymus. As described in the Experimental Section, this assay allows discrimination between nonspecific (due to intercalation) and specific (poisoning) effects on topoisomerase I by separation of various forms of plasmid DNA in agarose gels either without or containing ethidium bromide (Figure 8). Figure 8 clearly shows that camptothecin (CPT) as a potent poison of topoisomerase I strongly induced nicking of plasmid DNA, which can be seen as an increased intensity of the nicked open circular DNA band (cleavage product). On the other hand, ethidium bromide (EtBr) inhibited the relaxation of supercoiled DNA but did not induce nicking

of DNA. Being a strong intercalator, EtBr inserted itself between the stacked base pairs and thus inhibited DNA relaxation catalyzed by the enzyme (nonspecific, catalytic inhibitor). Furthermore, compound **11** induced nicking of plasmid DNA, pointing to the specific poisoning of topoisomerase I, although to a lesser extent than CPT, but it should be noted that the concentrations of both compounds were 100 μM, being extremely high for CMT, which is (as a specific topo I poison) active even in much lower concentrations. Compound **3** did not show specific topo I inhibitory effect at this concentration; however, it strongly inhibited topo I relaxation along with inducing topo I poisoning effect (enhanced nicking) at a concentration of 200 μM (Figure 8b). These results are substantiated by the analysis of the electrophoretic mobility of plasmid DNA in the agarose gel without EtBr, which is shown in Figure 8c, whereby the intensities of relaxed and nicked DNA are pronounced after incubation with both compounds, although some unwound (supercoiled) DNA is still present. On the other hand, intercalator EtBr completely inhibited the DNA relaxation, without causing relaxed and nicked products (see Supporting Information, Figure S3). Taken together, these results suggest that both compounds (**3**, **11**) act as catalytic topoisomerse I inhibitors and poisons, whereby compound **11** is either more specific or inhibits the activity of topoisomerase II and consequently induced DNA cleavage more strongly. The latter is substantiated by the above-discussed cell cycle influence experiments.

Conclusions

The spectrophotometric study revealed that nonfused benzimidazoles bind into minor groove of ds-DNA while their fused photoproducts intercalate into double-stranded polynucleotides. All studied compounds showed prominent growth inhibitory effect, whereby all fused compounds were more active than nonfused ones, most likely because of different modes of interaction with cellular DNA.

Among nonfused compounds, those containing thiophene moiety (**2**−**5**) were significantly more active than their furan-containing analogues. Furthermore, nonfused derivatives induced strong S phase arrest of the cell cycle followed by apoptosis that together with DNA minor groove binding mode pointed to topoisomerase I inhibition, which was additionally supported by the results of topoisomerase I unwinding/cleavage assay. In addition, all nonfused compounds revealed pronounced selectivity toward tumor cells in comparison with nontumor cells and therefore should be considered as promising lead compounds for further investigation.

On the other hand, fused analogues showed stronger but nondifferential activity, whereby imidazolyl-substituted compound **11** proved to be the most active one. Besides, it induced strong G2/M arrest of the cell cycle followed by drastic apoptosis, especially of HeLa cells.

Finally, it was shown that representatives of both nonfused (**3**) and fused (**11**) derivatives act as catalytic topoisomerse I inhibitors and poisons, whereby compound **11** as an intercalator revealed stronger activity than its nonfused analogue (**3**) acting as DNA minor groove binder. These results are in perfect agreement with the previously published ones,[31] which convincingly encourage further optimization and investigation of this lead structure.

Experimental Section

Chemistry. Melting points were determinate on a Koffler hot stage microscope. IR spectra were recorded on Nicolet magna 760,

Perkin-Elmer 297, and Perkin-Elmer Spectrum 1 spectrophotometers, with KBr disks. ^{1}H and ^{13}C NMR spectra were recorded on Varian Gemini 300, Bruker Avance DPX 300, and Bruker Avance DRX 500 spectrometers using TMS as an internal standard in DMSO-d_6. Elemental analysis for carbon, hydrogen, and nitrogen were performed on a Perkin-Elmer 2400 elemental analyzer and a Perkin-Elmer series II CHNS analyzer 2400. Where analyses are indicated only as symbols of elements, analytical results obtained are within 0.4% of the theoretical value. In preparative photochemical experiments the irradiation was performed at room temperature with a water-cooled immersion well with "Origin Hanau" 400 W high pressure mercury arc lamp using Pyrex glass as a filter. All compounds were routinely checked by TLC with Merck silica gel 60F-254 glass plates.

General Method for the Synthesis of *E-N*-Substituted 2-(2-Thiophen-2-ylvinyl)-3*H*-benzimidazole-5(6)-carboxamidine Hydrochlorides (2−5). A mixture of 3-thiophen-2-ylpropenal **1a**, the corresponding 4-*N*-substituted-1,2-phenylenediamines, and *p*-benzoquinone in absolute ethanol was stirred at reflux for 3 h under nitrogen. The reaction mixture was cooled at room temperature, diethyl ether was added, and the resulting solid was filtered off. The products were dissolved in ethanol and precipitated with diethyl ether, filtered off, and dried. It was repeated a few times until the products were analytically pure.

E-N-Isopropyl-2-(2-thiophen-2-ylvinyl)-3*H*-benzimidazole-5(6)-carboxamidine Hydrochloride (2). Compound **2** was prepared using the general method described above, from 3-thiophen-2-ylpropenal **1a** (0.200 g, 1.450 mmol), 4-*N*-isopropylamidno-1,2-phenylenediamine (0.331 g, 1.450 mmol), and *p*-benzoquinone (0.157 g, 1.450 mmol) in absolute ethanol (10 mL) after refluxing for 2 h to obtain 0.335 g (67%) of yellow-green powder; mp 291−293 °C. Anal. ($C_{17}H_{19}N_4ClS$) C, H, N.

E-6-(4,5-Dihydro-1*H*-imidazol-2-yl)-2-(2-thiophen-2-ylvinyl)-3*H*-benzimidazole Hydrochloride (3). Compound **3** was prepared using the general method described above, from 3-thiophen-2-ylpropenal **1a** (0.300 g, 2.171 mmol), 4-(2-imidazolinyl)-1,2-phenylenediamine (0.461 g, 2.171 mmol), and *p*-benzoquinone (0.234 g, 2.171 mmol) in absolute ethanol (15 mL) after refluxing for 3 h to obtain 0.717 g (88%) of gray powder; mp 178−180 °C. Anal. ($C_{16}H_{15}N_4ClS$) C, H, N.

E-N-Cyclohexyl-2-(2-thiophen-2-ylvinyl)-3*H*-benzimidazole-5(6)-carboxamidine Hydrochloride (4). Compound **4** was prepared using the general method described above, from 3-thiophen-2-ylpropenal **1a** (0.300 g, 2.171 mmol), 4-*N*-cyclohexylamidno-1,2-phenylenediamine (0.584 g, 2.171 mmol), and *p*-benzoquinone (0.234 g, 2.171 mmol) in absolute ethanol (15 mL) after refluxing for 2.5 h to obtain 0.630 g (75%) of light-green powder; mp >300 °C. Anal. ($C_{20}H_{23}N_4ClS$) C, H, N.

E-N-Morpholin-4-yl-2-(2-thiophen-2-ylvinyl)-3*H*-benzimidazole-5(6)-carboxamidine Hydrochloride (5). Compound **5** was prepared using the general method described above, from 3-thiophen-2-ylpropenal **1a** (0.300 g, 2.172 mmol), 4-*N*-morpholinylamidno-1,2-phenylenediamine (0.590 g, 2.172 mmol), and *p*-benzoquinone (0.234 g, 2.172 mmol) in absolute ethanol (15 mL) after refluxing for 2.5 h to obtain 0.650 g (77%) of green powder; mp >300 °C. Anal. ($C_{18}H_{20}N_5ClOS$) C, H, N.

General Method for the Synthesis of *E*-2-(2-Furan-2-ylvinyl)-*N*-substituted-3*H*-benzimidazole-5(6)-carboxamidine Hydrochlorides (6−9). A mixture of 3-furan-2-ylpropenal **1b**, the corresponding 4-*N*-substituted 1,2-phenylenediamines, and *p*-benzoquinone in absolute ethanol was stirred at reflux for 3 h under nitrogen. The reaction mixture was cooled at room temperature, and the resulting solid was filtered off. The products were dissolved in water and precipitated with acetone, filtered off, and dried. It was repeated two times until the products were analytically pure.

E-2-(2-Furan-2-ylvinyl)-*N*-isopropyl-3*H*-benzimidazole-5(6)-carboxamidine Hydrochloride (6). Compound **6** was prepared using the above described method, from 3-furan-2-ylpropenal **1b** (0.534 g, 4.381 mmol), 4-*N*-isopropylamidno-1,2- phenylenediamine (1.000 g, 4.381 mmol), and *p*-benzoquinone (0.474 g, 4.381 mmol) in absolute ethanol (20 mL) after refluxing for 2.5 h to obtain 0.700 g (50%) of gray powder; mp >300 °C. Anal. ($C_{17}H_{19}N_4OCl$) C, H, N.

6-(4,5-Dihydro-1*H*-imidazol-2-yl)-2-(2-furan-2-ylvinyl)-1*H*-benzimidazole Hydrochloride (7). Compound **7** was prepared using the above described method, from 3-furan-2-ylpropenal **1b** (0.401 g, 3.290 mmol), 4-(2-imidazolinyl)-1,2-phenylenediamine (0.700 g, 3.290 mmol), and *p*-benzoquinone (0.356 g, 3.290 mmol) in absolute ethanol (25 mL) after refluxing for 2 h to obtain 0.720 g (71%) of light-brown powder; mp 215−216 °C. Anal. ($C_{16}H_{15}N_4OCl_2 \cdot 3H_2O$) C, H, N.

E-N-Cyclohexyl-2-(2-furan-2-ylvinyl)-3*H*-benzimidazole-5-carboxamidine Hydrochloride (8). Compound **8** was prepared using the above described method, from 3-furan-2-ylpropenal **1b** (0.500 g, 4.100 mmol), 4-*N*-cyclohexylamidno-1,2- phenylenediamine (1.100 g, 4.100 mmol), and *p*-benzoquinone (0.443 g, 4.100 mmol) in absolute ethanol (25 mL) after refluxing for 2 h to obtain 0.950 g (70%) of gray powder; mp >300 °C. Anal. ($C_{20}H_{24}N_4OCl_2 \cdot H_2O$) C, H, N.

E-2-(2-Furan-2-ylvinyl)-3*H*-benzimidazole-5-carboxamidine Hydrochloride (9). Compound **9** was prepared using the above described method, from 3-furan-2-ylpropenal **1b** (0.500 g, 4.100 mmol), 4-amidino-1,2-phenylenediamine (0.764 g, 4.100 mmol), and *p*-benzoquinone (0.443 g, 4.100 mmol) in absolute ethanol (30 mL) after refluxing for 2 h to obtain 0.850 g (72%) of gray powder; mp >300 °C. Anal. ($C_{14}H_{13}N_4OCl \cdot 3H_2O$) C, H, N.

General Method for the Synthesis of *N*-Substituted 3-Thia-6,10b-diazacyclopenta[*c*]fluorene-8(9)-carboxamidine Hydrochlorides (10−13). A solution ($c = 1.3 \times 10^{-3}$ mol/dm^3) of corresponding *E-N*-substituted 2-(2-thiophen-2-ylvinyl)-3*H*-benzimidazole-5(6)-carboxamidine hydrochlorides (**2−5**) in ethanol was irradiated at room temperature with a 400 W high-pressure mercury lamp using a Pyrex filter for 6 h. The air was bubbled through the solution. The solution was concentrated and precipitated with diethyl ether, and the resulting solid was filtered off. After 2-fold recrystallization from ethanol/diethyl ether, pure products in the form of yellow powder were obtained.

N-Isopropyl-3-thia-6,10b-diazacyclopenta[*c*]fluorene-8(9)-carboxamidine Hydrochloride (10). Compound **10** was prepared as a mixture of two regioisomers, 85% of 8-position isomer (**10a**) and 15% of 9-position isomer (**10b**), using the general method described above, from *E-N*-isopropyl-2-(2-thiophen-2-ylvinyl)-3*H*-benzoimidazole-5(6)-carboxamidine hydrochloride (**2**) (0.100 g, 0.287 mmol) and iodine (0.005 g, 0.020 mmol) in ethanol (220 mL) after irradiation for 5 h to obtain 0.080 g (80%) of yellow powder; mp 210−211 °C. Anal. ($C_{17}H_{17}N_4ClS$) C, H, N.

8(9)-(1*H*-Imidazol-2-yl)-3-thia-6,10b-diazacyclopenta[*c*]fluorene Hydrochloride (11). Compound **11** was prepared as a mixture of two regioisomers, 85% of 8-position isomer (**11a**) and 15% of 9-position isomer (**11b**), using general method described above, from 6-(4,5-dihydro-1*H*-imidazol-2-yl)-2-(2-thiophen-2-ylvinyl)-3*H*-benzimidazole-5(6)-carboxamidine hydrochloride (**3**) (0.095 g, 0.291 mmol) and iodine (0.005 g, 0.020 mmol) in ethanol (220 mL) after irradiation for 6 h to obtain 0.069 g (73%) of yellow powder; mp 120−122 °C. Anal. ($C_{16}H_{13}N_4ClS$) C, H, N.

N-Cyclohexyl-3-thia-6,10b-diazacyclopenta[*c*]fluorene-8(9)-carboxamidine Hydrochloride (12). Compound **12** was prepared as a mixture of two regioisomers, 85% of 8-position isomer (**12a**) and 15% of 9-position isomer (**12b**), using the general method described above, from *N*-cyclohexyl-2-(2-thiophen-2-ylvinyl)-3*H*-benzimidazole-5-carboxamidine hydrochloride (**4**) (0.100 g, 0.260 mmol) and iodine (0.005 g, 0.020 mmol) in ethanol (220 mL) after irradiation for 6 h to obtain 0.070 g (71%) of yellow powder; mp 233−235 °C. Anal. ($C_{20}H_{21}N_4ClS$) C, H, N.

N-Morpholin-4-yl-3-thia-6,10b-diazacyclopenta[*c*]fluorene-8(9)-carboxamidine Hydrochloride (13). Compound **13** was prepared as a mixture of two regioisomers, 85% of 8-position isomer (**13a**) and 15% of 9-position isomer (**13b**), using the general method described above, from *N*-morpholin-4-yl-2-(2-thiophen-2-ylvinyl)-3*H*-benzimidazole-5-carboxamidine hydrochloride (**5**) (0.090 g, 0.231 mmol) and iodine (0.005 g, 0.020 mmol) in ethanol (220

mL) after irradiation for 6 h to obtain 0.060 g (67%) of yellow powder; mp 230−232 °C. Anal. ($C_{18}H_{18}N_5ClOS$) C, H, N.

Spectroscopy. The electronic absorption spectra were recorded on a Varian Cary 100 Bio spectrometer and CD spectra on a Jasco J815, in all cases using quartz cuvettes (1 cm). The measurements were performed in aqueous buffer solution (pH 7.0; sodium cacodylate buffer, $I = 0.05$ mol dm^{-3}). Under the experimental conditions used, the absorbance and fluorescence intensities of the studied compounds were proportional to their concentrations while none of studied compounds showed a CD spectrum. Fluorescence emission spectra were recorded on a Varian Eclipse fluorimeter (quartz cuvettes, 1 cm), from 350 to 550 nm and corrected for the effects of time- and wavelength-dependent light-source fluctuations using a standard rhodamine 101, a diffuser, and the software provided with the instrument. The sample concentration in fluorescence measurements had an optical absorbance below 0.05 at the excitation wavelength. Relative fluorescence quantum yields (Q) were determined according to the standard procedure used in previous work.[26] As the standard, we used *N*-acetyl-L-tryptophanamide (NATA) with published fluorescence quantum yield $Q = 0.14$.[26]

Interactions with Polynucleotides. Polynucleotides were purchased from Aldrich and dissolved in the sodium cacodylate buffer ($I = 0.05$ mol dm^{-3}, pH 7.0), and ct-DNA was additionally sonicated and filtered through a 0.45 μm filter. The concentration of polynucleotide solution was determined spectroscopically as the concentration of phosphates. Spectroscopic titrations were performed by adding portions of polynucleotide solution into the solution of the studied compound.

The stability constant (K_s) and [bound compound]/[polynucleotide phosphate] ratio (n) were calculated according to the Scatchard equation by nonlinear least-squares fitting, giving excellent correlation coefficients (>0.999) for obtained values for K_s and n.

Thermal melting curves for ct-DNA and polyA−polyU and its complexes with the studied compounds were determined as previously described[32] by following the absorption change at 260 nm as a function of temperature. The absorbance of the ligand was subtracted from every curve, and the absorbance scale was normalized. Obtained T_m values are the midpoints of the transition curves, determined from the maximum of the first derivative or graphically by a tangent method. Given ΔT_m values were calculated by subtracting T_m of the free nucleic acid from T_m of the complex. Every ΔT_m value here reported was the average of at least two measurements, and the error in ΔT_m is $\pm$ 0.5 °C. Viscometry experiments were conducted with an Ubbelohde microviscometer system. The temperature was maintained at 25 $\pm$ 0.1 °C. Aliquots of studied compound stock solutions were added to 5.5 mL of 5 × 10^{-4} M ct-DNA solution (pH 7, buffer Na cacodylate, $I = 0.05$ M), with ratio $r_{\text{[compound]/[ct-DNA]}} < 0.2$. The flow times were measured at least three times with a deviation of $\pm$0.5 s. The viscosity index α was obtained from the flow times at varying r according to the following equation:[42]

$$L/L_0 = [(t_r - t_0)/(t_{\text{DNA}} - t_0)]^{1/3} = 1 + \alpha r$$

t_0, t_{DNA}, and t_r denote the flow times of buffer, free DNA, and DNA complex at ratio $r_{\text{[1]/[ct-DNA]}}$, respectively, and L/L_0 is the relative DNA lengthening. The L/L_0 to r plot (Supporting Information) was fitted to a straight line that gave slope α. The error in α is $\pm$0.1. Under the same conditions, experiments with ethidium bromide (EB) were performed for comparison (Supporting Information).

Antitumor Activity Assays. Antiproliferative Activity. The HeLa (cervical carcinoma), Hep-2 (laryngeal carcinoma), MCF-7 (breast carcinoma), SW620 (colon carcinoma), and MiaPaCa-2 (pancreatic carcinoma) cells (obtained from American Type Culture Collection (ATCC, Rockville, MD)) were cultured as monolayers and maintained in Dulbecco's modified Eagle's medium (DMEM) supplemented with 10% fetal bovine serum (FBS), 2 mM L-glutamine, 100 U/mL penicillin, and 100 μg/mL streptomycin in a humidified atmosphere with 5% CO$_2$ at 37 °C. The growth inhibition activity was assessed as described previously, according to the slightly

modified procedure of the National Cancer Institute, Developmental Therapeutics Program.[10,26,31] Briefly, the cells were cultured as monolayers and maintained in Dulbecco's modified Eagle's medium (DMEM) supplemented with 10% fetal bovine serum (FBS), 2 mM L-glutamine, 100 U mL^{-1} penicillin, and 100 μg mL^{-1} streptomycin in a humidified atmosphere with 5% CO$_2$ at 37 °C. The cells were inoculated onto a series of standard 96-well microtiter plates on day 0, at 1×10^4 to 3×10^4 cells/mL, depending on the doubling times of specific cell line. Test agents were then added in five or 10-fold dilutions (10^{-8} to 10^{-4} M) and incubated for a further 72 h. Working dilutions were freshly prepared on the day of testing. The solvent was also tested for eventual inhibitory activity by adjusting its concentration to be the same as in the working concentrations. The cell growth rate was evaluated by performing the MTT assay after 72 h of incubation, which detects mitochondrial dehydrogenase activity in viable cells.

Each test was performed in quadruplicate in three individual experiments. The results are expressed as IC$_{50}$, which is the concentration necessary for 50% of inhibition. The IC$_{50}$ values for each compound are calculated from concentration−response curves using linear regression analysis by fitting the test concentrations that give PG values above and below the reference value (i.e., 50%). If, however, for a given cell line all of the tested concentrations produce PGs exceeding the respective reference level of effect (e.g., PG value of 50), then the highest tested concentration is assigned as the default value, which is preceded by a ">" sign.

Cell Cycle Analysis. The 2×10^5 cells were seeded per well into a six-well plate. After 24 h the tested compounds were added at various concentrations (as shown in the results section). After the desired length of time the attached cells were trypsinized, combined with floating cells, washed with phosphate buffer saline (PBS), fixed with 70% ethanol, and stored at −20 °C. Immediately before the analysis, the cells were washed with PBS and stained with 1 μg/mL of the propidium iodide (PI) with the addition of 0.2 μg/μL RNase A. The stained cells were then analyzed with Becton Dickinson FACScalibur (Becton Dickenson) flow cytometer (20 000 counts were measured). The percentage of the cells in each cell cycle phase was determined using the ModFit LT software (Verity Software House) based on the DNA histograms. The tests were performed in duplicate and repeated at least twice.

Detection of Apoptosis. Annexin-V Assay. Detection and quantification of apoptotic cells at the single cell level was performed using Annexin-V-FLUOS staining kit (Roche) according to the manufacturer's recommendations. The 2×10^4 cells were seeded per well into a 24-well plate. After 24 h the tested compounds were added at various concentrations (as shown in the results section). After the desired length of time, both floating and attached cells were collected. The cells were then washed with PBS, pelleted, and resuspended in staining solution (annexin-V-fluorescein labeling reagent and propidium iodide (PI) in Hepes buffer). The cells were then analyzed/counted under a fluorescence microscope. Annexin-V (green fluorescent) cells were determined to be apoptotic, and annexin-V and PI cells were determined to be necrotic. Percentage of apoptotic cells was expressed as a number of fluorescent cells in relation to the total cell number (fluorescent and nonfluorescent cells), which was expressed as 100%.[43]

Topoisomerase I DNA Unwinding/Cleavage Assay. In vitro assay using purified calf thymus topoisomerase I (Invitrogen) was used in order to check selected compounds for their inhibitory effect on topo I according to Bailly,[44] whereby two possible modes of inhibition can be detected: nonspecific effect due to DNA intercalation and specific effects resulting from the poisoning of topoisomerase I. Briefly, reaction mixture contained 0.8 μg of negatively supercoiled plasmid pCI (Promega, kindly provided by Dr. Andreja Ambriović Ristov, Rudjer Bošković Institute, Zagreb, Croatia) and 8 U of topoisomerase I with or without tested inhibitors in 40 μL of relaxation buffer (10 mM Tris-HCl, pH 7.5, 175 mM KCl, 5 mM MgCl$_2$, 0.1 mM EDTA, 2.5% glycerol). The mixtures were incubated at 37 °C for 30 min and reaction terminated by the addition of 2.5 μL of 10% SDS, followed by proteinase K (50 μg/

ml) digestion at 37 °C for 15 min. After extraction with a mixture of phenol, chloroform, and isoamyl alcohol (25:24:1), aqueous samples were removed and an amount of 4 μL of gel-loading buffer (0.25% bromphenol blue, 0.25% xylene cyanol, 60% glycerol, 150 mM Tris, pH 7.6) was added. The samples were divided into two and loaded onto either 1% agarose gel containing 0.5 μg/mL ethidium bromide or 1% agarose gel without ethidium bromide. Gels were run at 80 V constant voltage in a horizontal electrophoresis system (BIO-RAD). Resulting products were visualized and documented with UV light at 254 nm (Image Master VDS, Pharmacia Biotech, Sweden).

Supporting Information Available: Elemental analysis results, ^{1}H and ^{13}C NMR data, viscometry experiments, additional CD experiments, topoisomerase I inhibition assay. This material is available free of charge via the Internet at http://pubs.acs.org.

References

(1) Demeunynck, M.; Bailly, C.; Wilson, W. D. In *DNA and RNA Binders*; Wiley-VCH: Weinheim, Germany, 2002.

(2) Silverman, R. B. *The Organic Chemistry of Drug Design and Drug Action*, 2nd ed.; Elsevier Academic Press: Amsterdam, 2004.

(3) Martínez, R.; Chacón-García, L. The search of DNA-intercalators as antitumoral drugs: what worked and what did not work. *Curr. Med. Chem.* **2005**, *12*, 127–151.

(4) Brana, M. F.; Cacho, M.; Gradillas, A.; de Pascual-Teresa, B.; Ramos, A. Intercalators as anticancer drugs. *Curr. Pharm. Des.* **2005**, *7*, 1745–1780.

(5) Nelson, S. M.; Ferguson, L. R.; Denny, W. A. Non-covalent ligand/DNA interactions: minor groove binding agents. *Mutat. Res.* **2007**, *623*, 24–40.

(6) Baraldi, P. G.; Bovero, A.; Fruttarolo, F.; Preti, D.; Tabrizi, M. A.; Pavani, M. G.; Romagnoli, R. DNA minor groove binders as potential antitumor and antimicrobial agents. *Med. Res. Rev.* **2004**, *24*, 475–528.

(7) Bailly, C. Topoisomerase I poisons and suppressors as anticancer drugs. *Curr. Med. Chem.* **2000**, *7*, 39–58.

(8) Yang, X. L.; Wang, A. H.-J. Structural studies of atom-specific anticancer drugs acting on DNA. *Pharmacol. Ther.* **1999**, *83*, 181–215.

(9) Tanious, F. A.; Laine, W.; Peixoto, P.; Bailly, C.; Goodwin, K. D.; Lewis, M. A.; Long, E. C.; Georgiadis, M. M.; Tidwell, R. R.; Wilson, D. W. Unusually strong binding to the DNA minor groove by a highly twisted benzimidazole diphenylether: induced fit and bound water. *Biochemistry* **2007**, *46*, 6944–6956.

(10) Starčević, K.; Kralj, M.; Ester, K.; Sabol, I.; Grce, M.; Pavelić, K.; Karminski-Zamola, G. Synthesis, antiviral and antitumor activity of 2-substituted-5-amidino-benzimidazoles. *Bioorg. Med. Chem.* **2007**, *15*, 4419–4426.

(11) Ramla, M. M.; Omar, M. A.; Tokuda, H.; El-Diwani, H. I. Synthesis and inhibitory activity of new benzimidazole derivatives against Burkitt's lymphoma promotion. *Bioorg. Med. Chem.* **2007**, *15*, 6489–6496.

(12) Hoang, H.; LaBarbera, D. V.; Mohammed, K. A.; Ireland, C. M.; Skibo, E. B. Synthesis and biological evaluation of imidazoquinoxalinones, imidazole analogues of pyrroloiminoquinone marine natural products. *J. Med. Chem.* **2007**, *50*, 4561–4571.

(13) Cachoux, F.; Isarno, T.; Wartmann, M.; Altmann, K. H. Total synthesis and biological assessment of benzimidazole-based analogues of epothilone A: ambivalent effects on cancer cell growth inhibition. *ChemBioChem* **2006**, *7*, 54–57.

(14) Monem, A.; Abdel-Hafez, A. Benzimidazole condensed ring systems: new synthesis and antineoplastic activity of substituted 3,4-dihydro- and 1,2,3,4-tetrahydro-benzo[4,5]imidazo[1,2-*a*]pyrimidine derivatives. *Arch. Pharm. Res.* **2007**, *30*, 678–684.

(15) Ates-Alagöz, Z.; Alp, M.; Kus, C.; Yildiz, S.; Buyukbing, E.; Göker, H. Synthesis and potent antimicrobial activities of some novel retinoidal monocationic benzimidazoles. *Arch. Pharm. Chem. Life Sci.* **2006**, *339*, 74–80.

(16) Ates-Alagoz, Z.; Yildiz, S.; Buyukbingol, E. Antimicrobial activities of some tetrahydronaphthalene-benzimidazole derivatives. *Chemotherapy* **2007**, *53*, 110–113.

(17) Jayasekera, M. M. K.; Onheiber, K.; Keith, J.; Venkatesan, H.; Stocking, A. E. M.; Tang, L.; Miller, J.; Gomez, L.; Rhead, B.;

(18) Delcamp, T.; Huang, S.; Wolin, R.; Bobkova, E. V.; Shaw, K. J. Identification of novel inhibitors of bacterial translation elongation factors. *Antimicrob. Agents Chemother.* **2005**, 131–136.

(18) Morningstar, M. L.; Roth, T.; Farnsworth, D. W.; Smith, M. K.; Watson, K.; Buckheit, R. W., Jr.; Das, K.; Zhang, W.; Arnold, E.; Julias, J. G.; Hughes, S. H.; Michejda, C. J. Synthesis, biological activity, and crystal structure of potent nonnucleoside inhibitors of HIV-1 reverse transcriptase that retains activity against mutant forms of the enzyme. *J. Med. Chem.* **2007**, *50*, 4003–4015.

(19) Li, Y. F.; Wang, G. F.; Luo, Y.; Huang, W. G.; Chun-Lan Feng, W. T.; Shi, L. P.; Ren, Y. D.; Zuo, J. P.; Lu, W. Identification of 1-isopropylsulfonyl-2-amine benzimidazoles as a new class of inhibitors of hepatitis B virus. *Eur. J. Med. Chem.* **2007**, *42*, 1358–1364.

(20) Rida, S. M.; El-Hawash, S. A.; Fahmy, H. T.; Hazzaa, A. A.; El-Meligy, M. M. Synthesis of novel benzofuran and related benzimidazole derivatives for evaluation of in vitro anti-HIV-1, anticancer and antimicrobial activities. *Arch. Pharm. Res.* **2006**, *29*, 823–684.

(21) Velík, J.; Baliharová, V.; Fink-Gremmels, J.; Bull, S.; Lamka, J.; Skálová, L. Benzimidazole drugs and modulation of biotransformation enzymes. *Res. Vet. Sci.* **2004**, *76*, 95–108.

(22) Orjales, A.; Rubio, V.; Bordell, M. Benzimidazole Derivatives with Antihistaminic Activity. U.S. Patent 5877187, 1999.

(23) Göker, H.; Kus, C.; Boykin, D. W.; Yıldız, S.; Altanlar, N. Synthesis of some new 2-substituted-phenyl-1*H*-benzimidazole-5-carbonitriles and their potent activity against candida species. *Bioorg. Med. Chem.* **2002**, *10*, 2589–2596.

(24) Grogan, H. M. Fungicide control of mushroom cobweb disease caused by *Cladobotryum* strains with different benzimidazole resistance profiles. *Pest Manage. Sci.* **2006**, *62*, 153–161.

(25) Bielawska, A.; Bielawski, K.; Anchim, T. Amidine analogues of melphalan: synthesis, cytotoxic activity, and DNA binding properties. *Arch. Pharm. Chem. Life Sci.* **2007**, *340*, 251–257.

(26) Starčević, K.; Karminski-Zamola, G.; Piantanida, I.; Žinić, M.; Suman, L.; Kralj, M. Photoinduced switch of a DNA/RNA inactive molecule into a classical intercalator. *J. Am. Chem. Soc.* **2005**, *127*, 1074–1075.

(27) Jarak, I.; Kralj, M.; Suman, L.; Pavlović, G.; Dogan, J.; Piantanida, I.; Žinić, M.; Pavelić, K.; Karminski-Zamola, G. Novel cyano- and *N*-isopropylamidino-substituted derivatives of benzo[*b*]thiophene-2-carboxanilides and benzo[*b*]thieno[2,3-*c*]quinolones: synthesis, photochemical synthesis, crystal structure determination and antitumor evaluation. Part 2. *J. Med. Chem.* **2005**, *48*, 2346–2360.

(28) Tanious, F. A.; Hamelberg, D.; Bailly, C.; Czarny, A.; Boykin, D. W.; Wilson, W. D. DNA sequence dependent monomer–dimer binding modulation of asymmetric benzimidazole derivatives. *J. Am. Chem. Soc.* **2004**, *126*, 143–156.

(29) Wilson, W. D.; Nguyen, B.; Tanious, F.; Mathis, A.; Hall, J. E.; Stephens, C.; Boykin, D. W. Dications that target the DNA minor groove: compound design and preparation, DNA interactions, cellular distribution, and biological activity. *Curr. Med. Chem.: Anti-Cancer Agents* **2005**, *5*, 389–408.

(30) Mallena, S.; Lee, M. P. H.; Bailly, C.; Neidle, S.; Kumar, A.; Boykin, D. W.; Wilson, W. D. Thiophene-based diamidine forms a "super" AT binding minor groove agent. *J. Am. Chem. Soc.* **2004**, *126*, 13659–13669.

(31) Hranjec, M.; Kralj, M.; Piantanida, I.; Sedić, M.; Suman, L.; Pavelić, K.; Karminski-Zamola, G. Novel cyano- and amidino-substituted derivatives of styryl-2-benzimidazoles and benzimidazo[1,2-*a*]quinolines. Synthesis, photochemical synthesis, DNA binding and antitumor Evaluation. Part 3. *J. Med. Chem.* **2007**, *50*, 5696–5711.

(32) Piantanida, I.; Palm, B. S.; Eudić, P.; Žinić, M.; Schneider, H.-J. Interactions of acyclic and cyclic bis-phenanthridinium derivatives with ss- and ds-polynucleotides. *Tetrahedron* **2004**, *60*, 6225–6231.

(33) McGhee, J. D.; von Hippel, P. H. Erratum: theoretical aspects of DNA–protein interactions: co-operative and non-co-operative binding of large ligands to a one-dimensional homogeneous lattice. *J. Mol. Biol.* **1976**, *103*, 679.

(34) (a) Carlsson, C.; Larsson, A.; Jonsson, M.; Albinsson, B.; Norden, B. Optical and photophysical properties of the oxazole yellow DNA probes YO and YOYO. *J. Phys. Chem.* **1994**, *98*, 10313–10321. . (b) Furstenberg, A.; Deligeorgiev, T. G.; Gadjev, N. I.; Vasilev, A. A.; Vauthey, E. Structure–fluorescence contrast relationship in cyanine DNA intercalators: toward rational dye design. *Chem.–Eur. J.* **2007**, *13*, 8600–8609. (c) Deligeorgiev, T.; Vasilev, A. Cyanine Dyes as Fluorescent Non-Covalent Labels for Nucleic Acid Research. In *Functional Dyes*; Elsevier: Amsterdam, 2006; Chapter 4.

(35) Rodger, A.; Norden, B. In *Circular Dichroism and Linear Dichroism*; Oxford University Press: New York, 1997; Chapter 2.

(36) Berova, N.; Nakanishi, K.; Woody, R. W. *Circular Dichroism Principles and Applications*, 2nd ed.; Wiley-VCH: New York, 2000.

(37) Eriksson, M.; Nordén, B. Linear and circular dichroism of drug–nucleic acid complexes. *Methods Enzymol.* **2001**, *340*, 68–98.

(38) Wilson, W.D.; Ratmeyer, L.; Zhao, M.; Strekowski, L.; Boykin, D. The search for structure-specific nucleic acid-interactive drugs: effects of compound structure on RNA versus DNA interaction strength. *Biochemistry* **1993**, *32*, 4098–4104.

(39) Chen, A. Y.; Yu, C.; Gatto, B.; Liu, L. F. DNA minor groove-binding ligands: a different class of mammalian DNA topoisomerase I inhibitors. *Proc. Natl. Acad. Sci. U.S.A.* **1993**, *90*, 8131–8135.

(40) Cliby, W. A.; Lewis, K. A.; Lilly, K. K.; Kaufmann, S. H. S phase and G2 arrests induced by topoisomerase I poisons are dependent on ATR kinase function. *J. Biol. Chem.* **2002**, *277*, 1599–1606.

(41) Goldwasser, F.; Shimizu, T.; Jackman, J.; Hoki, Y.; O'Connor, P. M.; Kohn, K. W.; Pommier, I. Correlations between S and G2 arrest and the cytotoxicity of camptothecin in human colon carcinoma cells. *Cancer Res.* **1996**, *56*, 4430–4437.

(42) (a) Cohen, G.; Eisenberg, H. *Biopolymers* **1969**, *8*, 45. (b) Wirth, M.; Buchardt, O.; Koch, T.; Nielsen, P. E.; Nordén, B. *J. Am. Chem. Soc.* **1988**, *110*, 932. (c) Palm, B. S.; Piantanida, I.; Žinić, M.; Schneider, H.-J. *J. Chem. Soc., Perkin Trans. 2* **2000**, 385–392.

(43) Supek, F.; Kralj, M.; Marjanović, M.; Šuman, L.; Šmuc, T.; Krizmanić, I.; Žinić, B. Atypical cytostatic mechanism of N-1-sulfonylcytosine derivatives determined by in vitro screening and computational analysis. *Invest. New Drugs* **2008**, *26*, 97–110.

(44) Bailly, C. DNA relaxation and cleavage assays to study topoisomerase I inhibitors. *Methods Enzymol.* **2001**, *340*, 610–623.